European Conference on Optical Communication (ECOC) 2022 © Optica Publishing Group 2022

Research and Experiment on AI-based Co-cable and Co-trench Optical Fibre Detection

Yunbo Li(1), Chuan Li(2), Zhe Liu(2), Tao Zhang(2), Sheng Liu(1), Dawei Ge(1),Yuren You(2), Jibiao Zhang(2), Dong Wang(1), Yang Zhao(1), Dechao Zhang(1) ,and Han Li(1)

(1) Department of Fundamental Network Technology, China Mobile Research Institute, Beijing 100053, China, liyunbo@chinamobile.com
(2) Optical Architecture & Technology Planning Dept , Huawei Technologies Co., Ltd., Wuhan 430223, China

Abstract: *A novel AI-based co-cable and co-trench optical fibre detection method is proposed based on twin neural network and extraction of multimodal features, e.g. fibre static, dynamic, and site features. The detection accuracies of the solution in the test and field trial network are over 90%. ©2022 The Author(s)*

Introduction

Current optical cable resources are dumb, lacking in effective monitoring and O&M strategies, which actually allow primary and secondary services or associated services to be deployed on the same optical cable (co-cable). If a single optical cable used by both the primary and the secondary services becomes disconnected, both services would fail simultaneously. This leads to service interruptions and the potential for networks to become isolated. Co-cable information is maintained through manual line patrols and manual input. As the network changes, co-cable data in the resource management system becomes more complex, lagging and subsequently offers low co-cable identification efficiency and accuracy.

Optical fibres of a co-route (co-cable or co-trench) share the following features due to their close proximity and similar laying modes:

1. Similar optical fibre type and aging features [1-3], meaning the inherent static features of the fibres are similar.
2. Same or similar response to external vibration [4-8], meaning the dynamic features of the fibres are similar.
3. Close geographical proximity.

In this paper, we utilize the similar features shared by two fibres of a co-route, so that co-routes can be identified using AI technology based on static optical parameters, dynamic vibration features, and site location. The detection accuracies of the solution in the test and field trial network are over 90%.

Technical Principle of Proposed Solution

As we mentioned above, two optical fibres of a co-route should have similar static features, dynamic features, and site location features. Since the number of optical fibres in the fibre

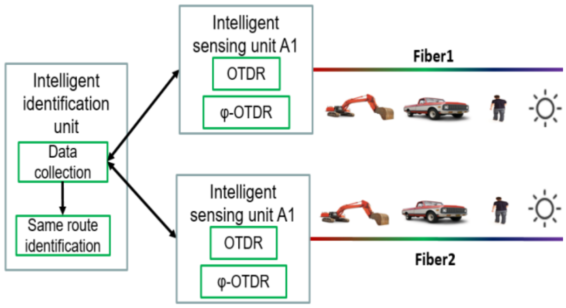

Fig. 1: The proposed solution architecture.

optic network is huge (at the magnitude of 10,000 or even 100,000), if only one feature is used as a determinant, it is very easy to misidentify a co-route. Therefore, in order to improve the detection accuracy of the system, a multimodal data fusion scheme is applied. Under the multimodal scheme, the entire transmission system deploys Intelligent Sensing Units (ISU) at the source and sink nodes of the optical section (OTS). The ISU can monitor a number of optical fibres simultaneously. The system also deploys an Intelligent Identification Unit (IIU) to implement co-route detection, as shown in Fig.1. The ISU can collect data measured by optical time domain reflectometer (OTDR), phase OTDR (φ-OTDR) in real time. It can perform millisecond-level collection of scattering features generated by fibre deterioration, fibre breakage, and fibre bending, as well as polarization features generated by running vehicles, excavation, and walking and running pedestrians. The large amount of data collected by ISU is compressed and extracted features using the twin neural network before sending them to the IIU. Finally, the co-route identification module in the IIU analyzes the fibre feature data to determine the co-route segments of the optical fibre.

In our solution, optical fibres are used as sensors to collect data. Fig. 2 shows the

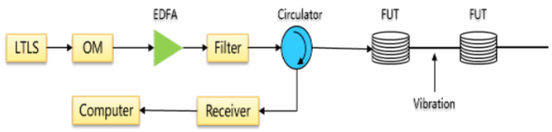

Fig. 2: Architecture of the Intelligent Sensing Unit.

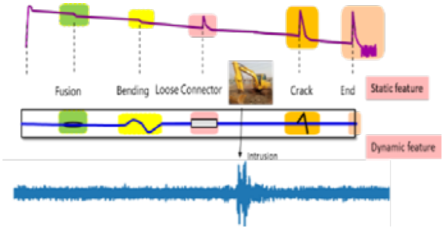

Fig. 3: Static and Dynamic Fibre Features.

hardware architecture of the ISU, including the three modules consisting of the transmitters (LTLS, OM, EDFA, and Filter), receiver, and computer.

The linewidth tunable light source (LTLS) can work in broadband mode or narrowband mode. When the LTLS works in broadband mode, as shown in Eq. (1), the slope of the detected Rayleigh scattering curve is related to fibre loss and can be used to detect fibre quality. When operating in narrowband mode, as shown in Eq. (2), interference occurs in the Rayleigh scattering, and when there is an external signal intruding, the phase of the interference signal changes due to the external intrusion and the change is linear to the intrusion signal. By using this relationship, the optical fibre can sense the external vibration and identify the dynamic features of the fibre.

$$I_r = \int_{-\pi}^{\pi} I_R(z) I_L \cos[\varphi_L - \varphi_R(z,t)] d\varphi_L = I_R(z) I_L \quad (1)$$

$$I_r = I_L I_R(z) \cos[\varphi_L - \varphi_R(z,t)] \quad (2)$$

where $I_R(z)/\varphi_R(z,t)$ is Rayleigh scattering echo intensity/phase, $I_L(z)/\varphi_L$ is local oscillator intensity/phase, I_r is echo intensity。

As shown in Fig. 3, the static feature of the optical fibre has greater attenuation at the points where the fibre is spliced or bent. When there is no external intrusion/disturbance, the signal obtained by the receiver is stable in the time domain. In the presence of external disturbances (knocking, excavating, vehicle running, etc.), the amplitude of signal fluctuation is visibly increased within the disturbed section of the optical fibre [8].

After receiving optical fibre features from the ISU, the IIU segments the fibre by a fixed length and uses a signal processing method and deep neural network to convert related data to the fibre's signature (fingerprint). By comparing fingerprint information of the fibre segment by segment, it becomes possible to determine whether the fibre shares a co-route with another fibre.

Co-route detection is a typical contrastive learning task that can be completed using the twin neural network architecture [9-10]. The twin neural network consists of two sub-networks that have the same structure and that share weights. Each sub-network contains *m* convolutional layers and *n* fully connected layers. By separately training the two sub-networks, eigenvectors and site geography information are obtained. A new eigenvector is then formed by concatenating this logical information. The degree of similarity between two fibres can then be found using the similarity matching layer.

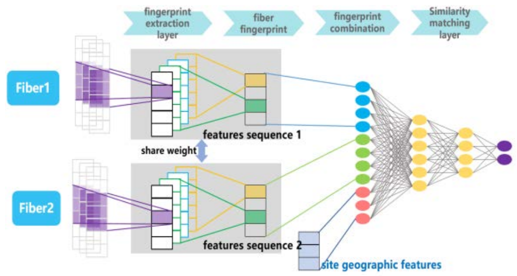

Fig. 4: Structure of Deep Twin Neural Networks.

As shown in Fig. 4, the input for the supervised twin neural network is data from static fibre features, dynamic fibre features, and site location features. The output label of co-routed fibres is set to '1' (positive), while the output label of non-co-routed fibres is set to '0' (negative). In the trial network, the data of manual/mechanical excavation, pedestrian walking, and vehicle driving under the soil conditions of sand, gravel, cement, etc. have been collected, but soil conditions/external vibration are more diverse in field trial networks. Due to the variance in different networks AI models encounter problems with generalization. Therefore, in the field, the model will first collect a small amount of fibre data and perform few-shot transfer learning on the pre-weighted neural network [11].

Experiment Verification

More than 100 scenarios were tested in the test site, featuring different burial depths (1.2 m to 2.4 m), distances (0 km to 50 km), soil textures (sand, soil, gravel, concrete), and fibre-optic wrapping materials (bare fibre, PVC, silicon core tube). Different external factors were also considered, for instance, rubber hammers may be used to strike the well wall or soil; pedestrians may walk and run in the test site; vehicles may drive through or idle in the test site; and excavation and mechanical tamping may be conducted in the test site.

Fig. 5 shows the waterfall diagram of events collected by ISUs on the field trial network, including manual excavation, vehicle driving, and excavator excavation. The x-axis corresponds to space and the y-axis corresponds to time elapsed.

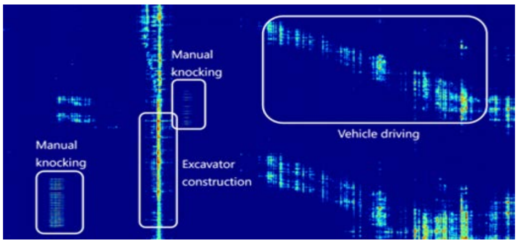

Fig. 5: Waterfall Diagram of Dynamic Features.

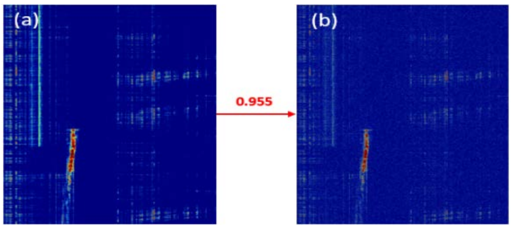

Fig. 6: Waterfall Diagrams of Features of Different Fibres in the Same Trench Section.

In manual excavation, labeled as "manual knocking", a shovel is used to dig on the ground. The vibration generated by the shovel will propagate in the direction of space and effect a segment of fiber, so the resulting output contains horizontal stripes. The excavator excavation event is labeled as "excavator construction" and generates an output at a fixed point in the figure, showing that the signal is bright relative to other signals in the figure because of stronger vibration. The output also displays relatively blurry horizontal stripes. One possible cause for this could be the impact from the vibration of the excavator's engine. Lastly, the "vehicle driving" event clearly shows the movement of the vehicle tracked through the dimensions of space and time elapsed.

Fig. 6(a) and 6(b) show waterfall diagrams generated by two fibre features in the same trench section, where Fig. 6(a) is one fibre feature located at a distance of about 10 km from the monitoring site A , and 6(b) is the other fibre feature at a distance of about 30 km from the monitoring site B. Although the signal-to-noise ratio in 6(b) is lower than that of 6(a), the degree of similarity between the two images is 0.955 and the excavator excavation and vehicle driving events can still be recognized.

Fig. 7 show waterfall diagrams generated by fibre features that are not in the same trench section. The subfigures (a-f) show events such as vehicles driving and excavator driving; however, the events are distributed in different geographical locations, so the features of the various events are dissimilar.

Our scheme has been verified in the test and field trial network, the results are summarized in Table 1.

A、In test trial network，a total of 5948 test cases were run, of which 588 cases involved co-

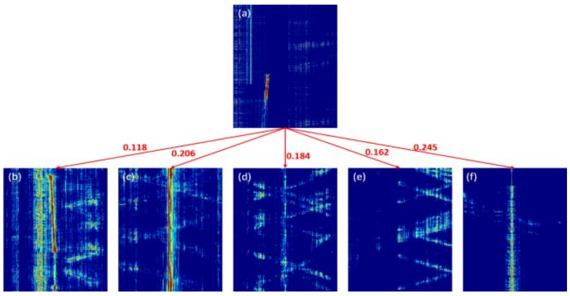

Fig. 7: Waterfall Diagrams of Features of Different Fibres in Different Trench Sections.

Tab. 1: Confusion Matrix for Co-Route Detection

Confusion Matrix			Predict	
			Positive	Negative
Test Trial Network	Actual	Positive	541	47
		Negative	24	5336
Field Trial Network	Actual	Positive	367	34
		Negative	2	180

Note: Positive – co-routed fibre pairs, Negative: non-co-routed fibre pairs.

routed fibres and 5360 cases involved non-co-routed fibres. 541 co-routed fibre test cases were successfully identified, and 47 cases remained undetected, the correct detection rate is 92.0%. 24 non-co-routed fibre were wrongly identified, the false positive rate is 0.45%.

B、In filed trial network，583 test cases were run, of which 401 cases involved the same trench section and 182 cases involved different trench sections. Test results show a detection rate of 91.52% and a false positive rate of 1.1%, which preliminarily proves the feasibility and effectiveness of the solution.

Conclusion

The isolation of primary and secondary routes is critical for ensuring communication reliability. However, traditional optical cable resources rely on manual operations, which is inefficient, costly, and fails to provide dynamic service. This paper proposes a new optical fibre co-route detection technology to serve as a Shared Risk Link Group intelligent identification solution. The technology uses a multimodal data analysis architecture to precisely extract the static, dynamic, and site location features of fibres. The twin neural network is then used for implementing intelligent detection of a co-route. The detection rate on the field trial network is greater than 90%, offering higher detection accuracy and efficiency than the traditional manual method.

Acknowledgments

This work was supported by National Key Research & Development Program of China (No. 2019YFB1803605).

References

[1] M. Ohashi, H. Kubota, Y. Miyoshi, R. Maruyama, and N. Kuwaki, "Longitudinal fiber parameter measurements of two-mode fiber links by using OTDR", *European Conference on Optical Communication (ECOC 2013)*, Th.1.4.5, Cannes, France, 2013. DOI: https://doi.org/10.1109/ECOC.2014.6964168

[2] H. Iida, H. Hirota, T. Uematsu, K. Noto, "Fresnel reflection analysis for optical fibre identification employing with three-wavelength OTDR", *European Conference on Optical Communications (ECOC 2020)*, Tu1J-8, Brussels, Belgium, 2020. DOI: https://doi.org/10.1109/ECOC48923.2020.9333328

[3] M. Ohashi, A. Nakamura, T. Oda, K. Hayakawa, and Y. Koshikiya, "Measurement of fiber parameters of pure silica core fibers based on the OTDR technique", *Optics Express*, vol. 29, no. 10, pp. 15078-15088, 2021. DOI: https://doi.org/10.1364/OE.424706

[4] T. Okamoto, D. Iida, Y. Koshikiya, N. Honda, "Distributed Vibration Sensing of Seismic Event by Optical Frequency Domain Reflectometry", *European Conference on Optical Communication (ECOC 2021)*, Tu2C1.3, Bordeaux, France, 2021. DOI: https://doi.org/10.1109/ECOC52684.2021.9605954

[5] Y. Wei, Y. E. Li, J. Zong, J. Yang, H. Fu, M. Sun, "Deep learning-based P-and S-wave separation for multi-component Vertical Seismic Profiling", *IEEE Transactions on Geoscience and Remote Sensing*, vol. 60, no. 5908116, 2021. DOI: https://doi.org/10.1109/TGRS.2021.3124413

[6] A. Venketeswaran, N. Lalam, J. Wuenschell, P. R. Ohodnicki Jr., M. Badar, K. P. Chen, P. Lu, Y. Duan, B. Chorpening, M. Buric, "Recent Advances in Machine Learning for Fiber Optic Sensor Applications", *Advanced Intelligent Systems*, vol. 4, no. 1, pp. 1-24, 2022. DOI: https://doi.org/10.1002/aisy.202100067

[7] M. Aktas, T. Akgun, M. U. Demircin, D. Buyukaydin, "Deep learning based multi-threat classification for phase-OTDR fiber optic distributed acoustic sensing applications", *Fiber Optic Sensors and Applications XIV. International Society for Optics and Photonics*, vol. 10208, no.1, 2017. DOI: https://doi.org/10.1117/12.2262108

[8] Y. Yang, Y. Li, T. Zhang, Y. Zhou, H. Zhang, "Early safety warnings for long-distance pipelines: A distributed optical fiber sensor machine learning approach", Proceedings of the AAAI Conference on Artificial Intelligence, vol. 35, no. 17, pp. 14991-14999, 2021. DOI: https://ojs.aaai.org/index.php/AAAI/article/view/17759

[9] H. Jiang, X. Hu, K. Li, J. Zhang, J. Gong, M. Zhang, "PGA-SiamNet: Pyramid feature-based attention-guided siamese network for remote sensing orthoimagery building change detection", *Remote Sensing*, vol.12, no.3, pp. 484, 2020. DOI: https://doi.org/10.3390/rs12030484

[10] A. He, C. Luo, X. Tian, W. Zeng, "A twofold siamese network for real-time object tracking", *2018 IEEE/CVF Conference on Computer Vision and Pattern Recognition (CVPR 2018)*, pp. 4834-4843, Salt Lake City, USA, 2018. DOI: https://doi.org/10.1109/CVPR.2018.00508

[11] F. Sung, Y. Yang, L. Zhang, T. Xiang, P. H. S. Torr, T. M. Hospedales, "Learning to compare: Relation network for few-shot learning", *2018 IEEE/CVF Conference on Computer Vision and Pattern Recognition (CVPR 2018)*, pp. 1199-1208, Salt Lake City, USA, 2018. DOI: https://doi.org/10.1109/CVPR.2018.00131